Wrinkling prediction, formation and evolution in thin films adhering on polymeric substrata

A. Cutolo [a,1], V. Pagliarulo [b,1], F. Merola [b,1], S. Coppola [b], P. Ferraro [b,*], M. Fraldi [a,b]

[a] Department of Structures for Engineering and Architecture, University of Napoli Federico II, Napoli, Italy
[b] Institute of Applied Sciences and Intelligent Systems (CNR-ISASI), National Research Council of Italy, Via Campi Flegrei 34, 80078 Pozzuoli (NA), Italy

HIGHLIGHTS

- We investigated the experimental formation of wrinkled patterns achieved on periodic structures;
- Different parameters (substrates, coating metals and shapes) have been analysed;
- Hybrid analytical-numerical strategy for predicting the onset, evolution of wrinkling in metal film on 3D-shaped substrates.
- The results might be helpfully utilized for predicting hierarchical organizations of wrinkle patterns

GRAPHICAL ABSTRACT
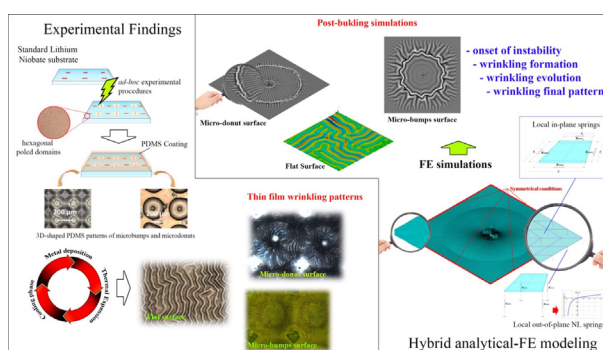
ABSTRACT

Wrinkling has recently attracted an increasing interest by suggesting a number of unforeseeable applications in many emerging material science and engineering fields. If guided and somehow designed, wrinkles could be in fact used as an alternative printing way for realizing complex surface geometries and thus employed as an innovative bottom-up process in the fabrication of nano- and micro-devices. For these reasons, the prediction of wrinkles of films adhering on flat as well as on structured substrata is a challenging task, genesis and development of the phenomenon being not yet completely understood both when thin membranes are coupled with soft supports and in cases where the geometry of the surfaces are characterized by complex three-dimensional profiles. Here we investigate the experimental formation of new intriguing and somehow unforeseeable wrinkled patterns achieved on periodic structures, by showing prediction through a new hybrid analytical-numerical strategy capable to overcome some common obstacles encountered in modeling film wrinkling on flat and 3D-shaped substrata. The proposed approach, which drastically reduces the computational effort, furnishes a helpful way for predicting both qualitative and quantitative results in terms of wrinkling patterns, magnitude and wavelength, by also allowing to follow the onset of film instabilities and the progressive evolution of the phenomenon until its final stage.

© 2018 The Authors. Published by Elsevier Ltd. This is an open access article under the CC BY-NC-ND license (http://creativecommons.org/licenses/by-nc-nd/4.0/).

1. Introduction

Wrinkles at micro- and nano-scale have found applications in surprising ways in many emerging fields [1–8]. Spontaneous wrinkled micro-patterns are generally formed in compressed thin metal films attached

* Corresponding author.
  E-mail address: p.ferraro@isasi.cnr.it (P. Ferraro).
[1] These authors contributed equally.

to a thicker compliant substrate in a variety of situations. Understanding how they form and develop is very attractive also because their use could be oriented to create specific profiles avoiding additive manufacturing processes [9]. Recently, it has been for instance shown that wrinkle patterns can be very useful as photonic structures in photovoltaics [10] with the aim of improving the efficiency in the near-infrared region, or to enhance the energy conversion efficiency (ECE) [11]. Moreover, in the field of opto-electronics [3,5,8], the wrinkles have been exploited to enhance the luminescence of organic light emitting diodes (OLED) [12], suggesting potential applications in photodetectors [1], solar cells [8,13], soft actuators [5], pressure sensors [2], many further perspectives being foreseen for flexible electronic devices [3,14]. Possible uses have been also highlighted in biological and biomedical applications [4] and in low-threshold stretchable random lasers as well [6].

As mentioned above, surface patterning by wrinkling generally occurs spontaneously, driven by mechanical or thermal-induced stresses [15]. In particular, the wrinkling effect was deeply investigated in the case of soft materials. Polymeric materials [4,16,17] such as Polydimethylsiloxane (PDMS) [18–20] give rise to a wrinkled patterns by depositing a thin metal layer on the polymer stratum. Bowden et al. [21] described one of the first evidence of such phenomena in a typical experimental procedure in which a metal film, deposited on the top of polymeric substrates by means of electron-beam evaporation techniques, is finally deformed. In this case, the warmer metal heats and expands the support whereas it - in a liquid/solid transition state - undergoes thermal expansion, maintaining a stress-free state and deforming together with the substrate [1]. Thereafter, the sample is cooled and the solidifying film, under compressive stress, buckles by bringing the entire system in the lowest energy configuration [18]. In another case, the wrinkling phenomena have been treated as an undesirable effect in layered structure because of their uncontrollability [22]. It was also explored the possibility to have wrinkling formation without the use of metal layers. For instance, Yang et al. utilized a combination of external straining and selective O_2 plasma exposure to control the surface wrinkling [23], by adopting a copper grid to define the wrinkled area. Other chemical techniques have been successfully adopted in the wrinkles formation [24]. As it can be easily guessed, a different type of polymer, as well as different thermomechanical stresses, can all lead to a vast variety of wrinkling patterns [15,23,25]. Recently, instability phenomena involving liquid crystals [26] and graphene adopted for flexible electronics [3] and other technological applications [27–29] have been also investigated.

Different fabrication techniques have been used for wrinkles formation [30,31], by analyzing patterns, characteristic wavelength [32–35] and the instabilities onset [36,37]. Reversible wrinkles generation process has also been demonstrated [38] even if the quantitative prediction and the tracing of the whole pattern evolution on curved surfaces - that would represent a potential way to facilitate the design of functional materials and structures by harnessing these surface instabilities [39] - are still challenging due to strong nonlinearities and geometric complexities involved in any numerical modeling. Such structures are also at the center of a vivid debate for the evidence that they can be exploited as efficient optical micro-lenses and photonics tools in different configurations and then helpfully adopted for different purposes and applications [40], the micro-lenses for example permitting to combine two optical functionalities in just one optical element.

Motivated by this wide interest in the field, here we investigate the formation of film wrinkling on both polymeric flat surfaces and substrata characterized by three-dimensional periodic profiles induced by means of pyroelectric-Dielectrophoresis (pyro-DEP) [41–43]. In particular, we studied and experimentally induced the formation of such wrinkles on non-flat surfaces, by showing that a number of possible interesting "horographies" can be drawn by playing on how the three-dimensional shape of the substrate on which the films adhere influences and somehow orients the wrinkling pattern. Since a faithful prediction of such phenomena is crucial if one needs to "design" these wrinkled structures by following an alternative way to micro-printing strategies [44], we also proposed a novel hybrid analytical-numerical approach which, by implementing in a Finite Element-based algorithm a mechanically nonlinear model of the elastic substrate made up of an ad hoc three-dimensional network of nonlinear springs, allows to drastically reduce computational costs and to capture with sufficiently good accuracy the whole wrinkling process, from its formation to its progression and final stabilization. The agreement between numerical outcomes and experimental results related to the wrinkling of films on flat and different non-flat surfaces is in detail shown and critically discussed.

2. Methodology

2.1. Experimental process for fabrication of elastic substrates with wrinkles patterns on complex structures

For the fabrication of the polymer substrate we have here exploited the well-known properties of periodically poled Lithium Niobate crystals (PPLN) [45,46]. With this respect, PPLN has been recently used as substrate for elastomers and for driving the formation of well-ordered and arrayed protruding structures created by the so-called pyro-DEP. We therefore used such geometrical polymeric structures as basis for achieving particular and fascinating nano-wrinkles standing on this complex non-flat surfaces. Two different substrates were in particular employed for the experimental tests, i.e. a plain glass plate and a $LiNbO_3$ substrate, the glass being just adopted as control and as preliminary samples in order to understand and calibrate the system.

A micro-engineering process made of two steps - a conventional photolithography and a standard periodic electric field poling - was carried out onto polished z-cut 500 μm thick LN substrates (Crystal Technology Inc.) in order to get the above mentioned PPLN. The full process, described in details in Supporting Informations, affects the structure of the Lithium Niobate sample, which assumes a square array of hexagonal reversed domains, as shown in Fig. 1(a). As illustrated in previous works, the use of PPLN as substrate of PDMS layers allows to obtain very interesting well-ordered patterns, simply by rapidly heating the sample on a hot plate and suddenly cooling it [47–50]. An example of the built up three-dimensional structure is shown in Fig. 1 (b, c), where sub-hemispherical (b) [41] or sub-toroidal ring-shaped (c) structures [47] occur. Moreover, a profilometer analysis has been conducted to highlight the height profile of the two structures in Fig. 1 (b, c) and the result is reported in Fig. 1(d, e).

Successively, such structures were coated with metal through the process illustrated and summarized in Fig. 2, the final result being the formation of 3D complex wrinkled patterns onto the surface (details can be found in the Supporting Information).

In Fig. 3 are reported images at the microscope of two samples in which Al has been used as coating, one showing a region of the sample with micro-bumps (Fig. 3a and b) and the other the micro-doughnuts (Fig. 3c and d). As it is clearly visible, the wrinkles follow particular patterns by circumventing the regions in correspondence of the hexagons in case of micro-bumps (see Fig. 3(a, b)) by instead occurring inside the ring in the case of micro-doughnuts (see Fig. 3(c, d)) at the opposing faces of the PPLN substrate. In both such geometries, typically the wrinkles have wavelength of 10–15 μm and a height of about 0.5 μm. It is worth to highlight that the shape of the underlying hexagonal domains of then PPLN is still easily visible.

In the second experiment, we adopted Au as coating metal. In this case the patterns were found as very regular, by also showing a "scaling-down" of their dimensions. How the PDMS structures influenced the wrinkles formation is quite evident in the case of Fig. 4(a–d), where the shape of the hexagonal domains is easily visible thanks to the spatial distribution and the localization of the wrinkles. To highlight the results, the specimen illustrated in Fig. 4 was also illuminated with a HeNe laser (@633 nm) and the interesting diffraction pattern is shown in the inset of Fig. 4a.
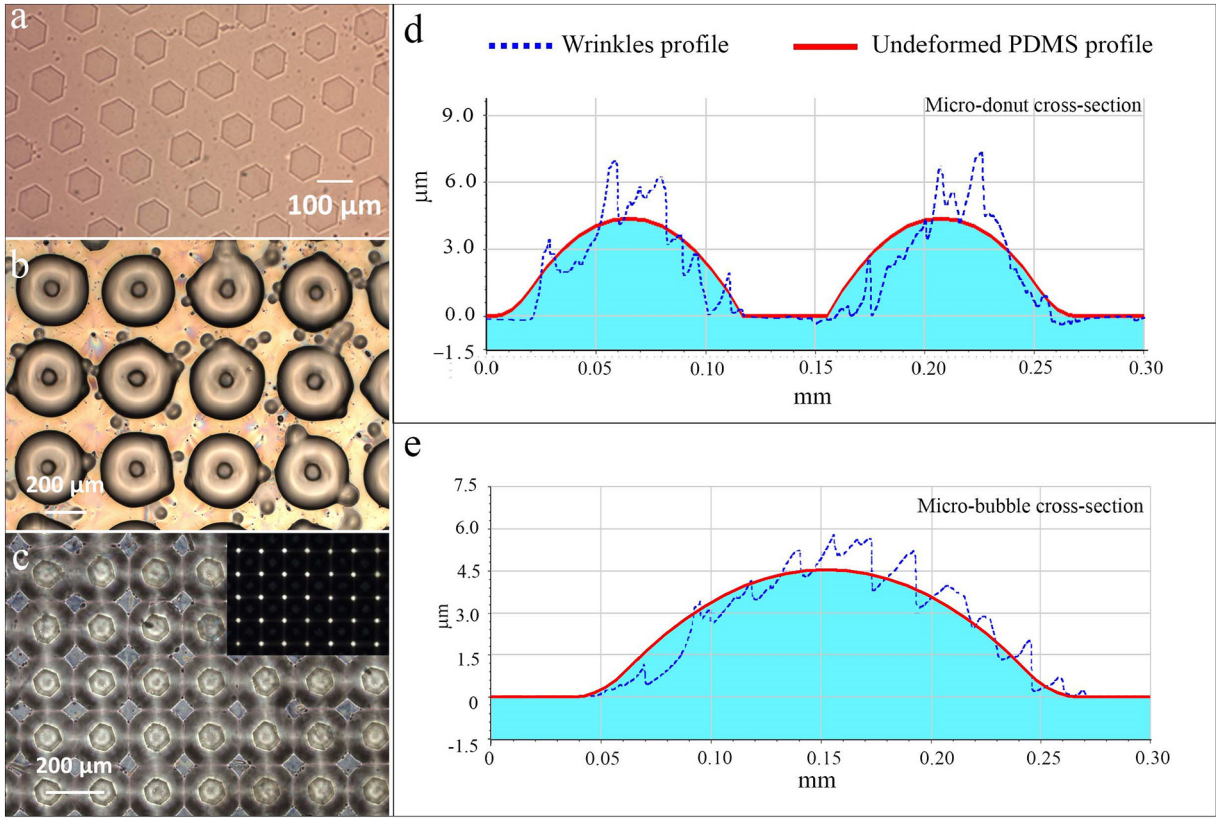
Fig. 1. (a)Periodically poled LN (PPLN) substrate (b) PDMS micro-bumps array on Z+ side of the PPLN crystal, in the inset the focal plane is shown. (c) PDMS doughnut array on PPLN Z− side. (d, e) Height profile of the PDMS substrate (red line) and wrinkles profile (blue dotted line); (d) doughnuts, (e) bumps. (For interpretation of the references to colour in this figure legend, the reader is referred to the web version of this article.)

Independently from other geometrical and thermo-mechanical parameters that will be analyzed below through the in silico simulations, it appears as evident that the difference in wrinkling wavelengths between Al and Au samples is associated to the different metal thickness. In fact, it can be argued that higher metal thicknesses leads to larger wrinkles wavelengths due the cooperation of geometrical and mechanical parameters, which in turn can kindle greater thermal stresses. However, the interplay among the geometric characteristics and the thermo-mechanical properties of the film-substrate system governs the wrinkles formation [51]. In fact, by looking at the results found in the literature, Bowden et al. [21], with 1 cm of PDMS on glass and 50 nm of Au, coherently obtained a wavelength of about 20 μm: as a consequence, by changing materials and geometries and applying (or inducing) different stress levels, one could obtain wrinkles wavelengths from hundreds μm down to hundreds nm [52,53], in this manner paving the way for a controlled design of the wrinkling patterns. Therefore, with the aim of giving a predictive tool for anticipating the geometry of the wrinkled surface and to envisage alternative strategies to 3D printing, in what follows we develop and test a hybrid analytical-numerical approach for simulating the response of thin films adhering on flat and non-flat surfaces, by showing the accuracy of the outcomes and the robustness of the proposed method for possible future applications.

2.2. Problem assessment

Several works have been focused on the role played by the stiffness mismatch of coupled materials on the surface wrinkling patterns. Nowadays the motivations for studying these non-linear phenomena have arisen due to the wide innovative applications occurring at different scales [54,55] and, with the aim to predict and control the wrinkling formations, a large literature exists reporting both analytical and numerical approaches [56].

To analytically model wrinkling phenomena and gain qualitative and quantitative insights into amplitudes and wavelengths of films adhering to deformable supports, some hypotheses are usually introduced by considering the substrate infinitely depth and the elastic film in plane-strain conditions. If the deposition is assumed to occur at uniform temperature T_D and the drop temperature ΔT is applied for inducing compressive stress states, the wrinkling is essentially governed by the mismatch between the thermal expansion coefficients of substrate and film, $\Delta\alpha = \alpha_s - \alpha_f$, and the mean value of the equi-biaxial compressive stress in the film, σ_0, can be evaluated by means of the Equation [57]:

$$\sigma_0 = (E_f/1 - \nu_f)\Delta\alpha\Delta T \tag{1}$$

where E_f and ν_f are the Young's modulus and the Poisson's ratio of the film, respectively (the corresponding coefficients for the substrate being E_s and ν_s), and α_s and α_f are the thermal expansion coefficients of support and film. In this way, the instability is triggered by a *dormant* plane strain, characterizing the early stage of the monotonic deformation process, followed by an out-of-plane film bending that can be well described by the *Foppl-von Karman* equations [5]. By linearization of these equations, the problem reduces to seek eigenvalues and eigenvectors that finally permit to estimate both the critical compressive load at which the film buckles and the wrinkling wavelength as functions of geometrical and material properties of the system, through the formulas [58,59]:

$$\sigma_0^C = 3^{\frac{2}{3}}/4\left((E_s/1 - \nu_s^2)^{\frac{2}{3}}(E_f/1 - \nu_f^2)^{\frac{1}{3}}\right), \tag{2}$$

$$\lambda_0^C = 2\pi t(E_f(1 - \nu_s^2)/3(1 - \nu_f^2)E_s)^{\frac{1}{3}}$$

The *critical* drop temperature ΔT_c needed to produce the compressive stress at which the first bifurcation of equilibrium occurs, thus
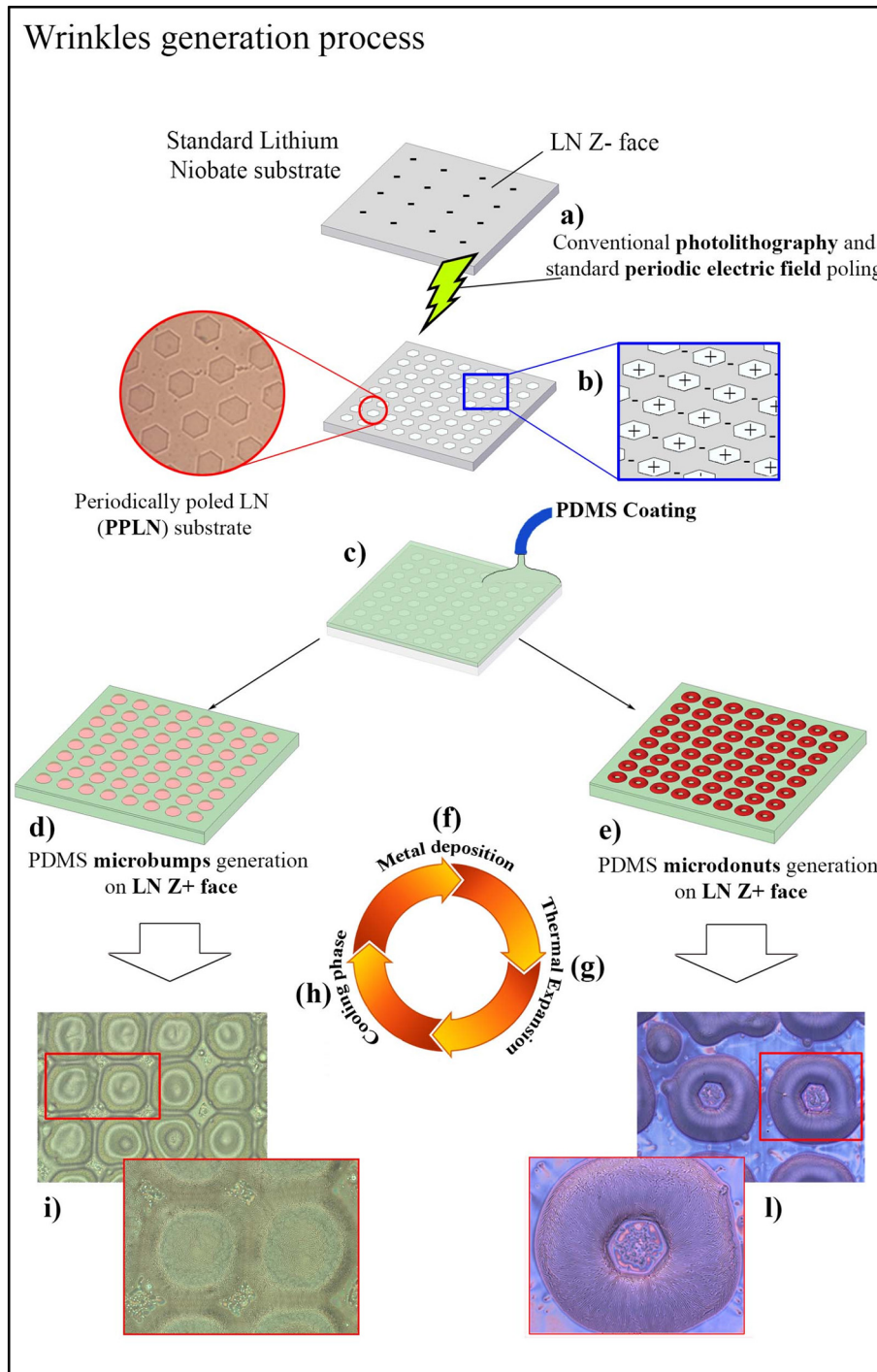
Fig. 2. PDMS wrinkles generation process. (a) A lithium niobate substrate is micro-engineered to obtain (b) reversed hexagonal domains. (c) A film of PDMS is spin-coated on the substrate (both sides) and heated generating arrays of micro-bumps (d) and micro-doughnuts (e). (f) A thin layer of metal is deposited a PDMS substrate during a heating cycle (g), successively the system is cooled (h), thus resulting in the generation of a compressive stress state leading to wrinkles formation. Wrinkles generated on the (i) Z+ and (l) Z− side of the crystal.

inducing wrinkling, can be obtained by equating the in situ stress to the critical one as [59,60]

$$\sigma_0 = \sigma_0^C \quad \Rightarrow \quad \Delta T_c = \frac{3^{\frac{2}{3}}\left(1-\nu_f\right)\left(\left(E_s/1-\nu_s^2\right)^{\frac{2}{3}}\left(E_f/1-\nu_f^2\right)^{\frac{1}{3}}\right)}{4E_f\Delta\alpha} \quad (3)$$

Although the above recalled formulas can be effectively used to roughly estimate the onset of instability in simpler cases, they are however insufficient to predict formation and progressive evolution of wrinkling when the meddling of non-homogenous boundary conditions, non-flat shape of the substrate, material and geometrical nonlinearities lead to combined modes which draw complex out-of-plane deformation patterns. Actually, both substrate nonlinearity and pre-stretch could influence the instability onset and the evolution and the shape of the wrinkling modes as compression increases beyond the critical bifurcation load [55,61]. 2D and 3D models have been addressed in literature, where computational strategies based on numerical algorithm [62] or making use of Finite Element-based codes to perform numerical analyses [60,63–67] have been adopted. However, in silico
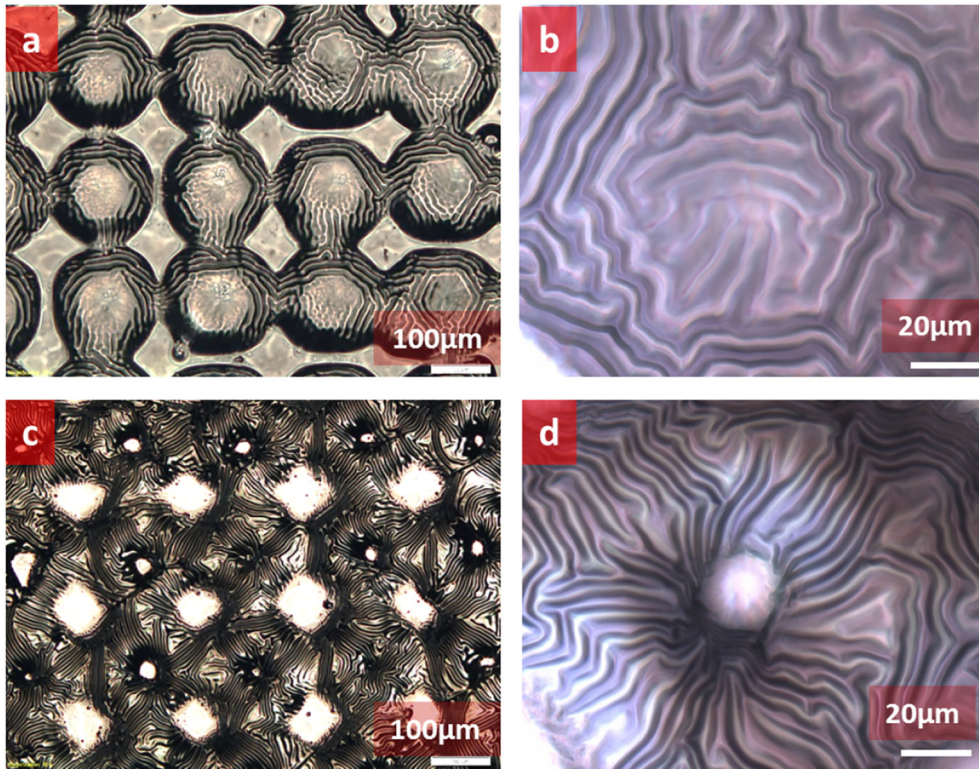
Fig. 3. Microscope images of Al wrinkles formation on (a, b) PDMS microbumps and (c, d) doughnuts, with different magnification.

simulating with sufficient accuracy wrinkling in three-dimensional film-substrate systems is to date still a difficult task, the analyses being significantly prevented by the need to generate mesh with an extremely large number of elements to compensate the size discrepancy between the thicknesses of the thin film and of the thick (bulky) substrate. In this framework, several approaches have been indeed
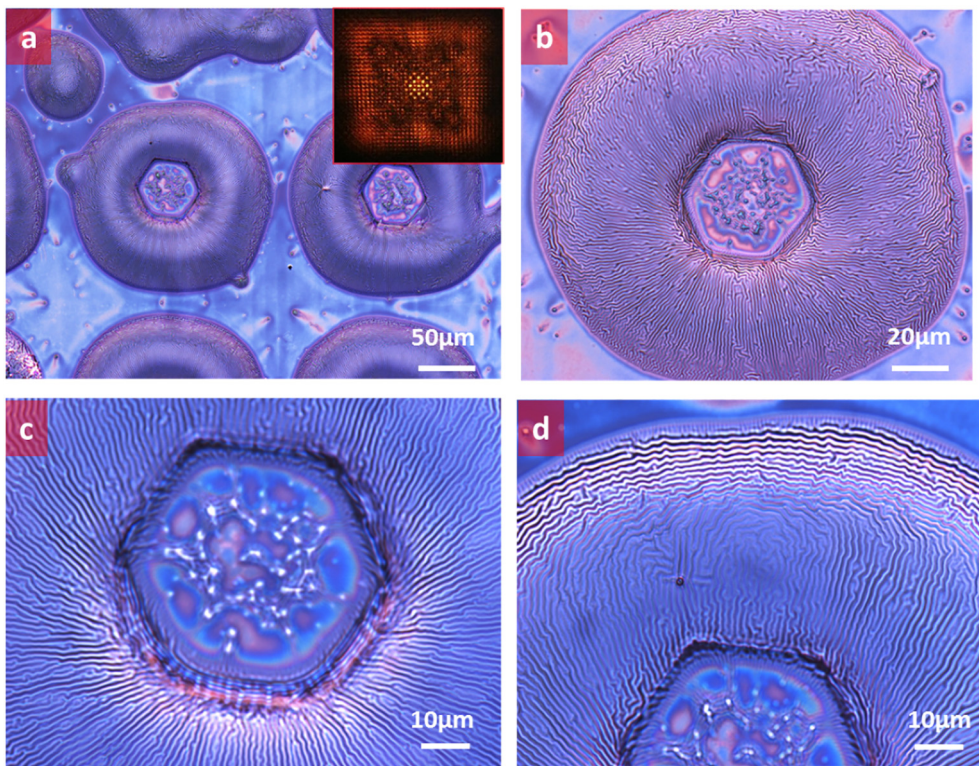

Fig. 4. Microscope images of Au wrinkles formation on PDMS doughnuts, with different magnification (higher from *a* to *d*). The pattern is more regular and with reduced pitch, compared to the case of Al as top metal. The inset of (a) represents the diffraction pattern generated by the sample illuminated by a He—Ne laser beam thus showing the quite uniform periodic nature of the wrinkle patterns.

addressed to limit computational costs [65]. More in general, wave patterns also depend on the bas-relief present on the surface substrate and therefore the numerical routines have to be ad hoc designed to capture unexpected transitions from random nucleation of swollen loci and disordered deformation modes to strongly ordered wave patterns [68,69], as observed during the formation of micro- and nano-wrinkling in thin metal film adhering to irregular elastic supports [59,64,69–71]. However, as a matter of fact, only relatively few literature works have been spent so far to characterize numerically the unstable behavior of thin film bonded to an irregular non-flat substrates [67,72,73].

2.3. Hybrid analytical-numerical approach for thin films wrinkling on elastic substrates

To overcome the intrinsic computational limitations of the previous approaches and faithfully simulating the nonlinear post-buckling behavior of thin layers adhering on a bulky elastic substrate with possible surface bas-relief is still a challenging task [66].

A thin shell representing the metal film deposited on a polymeric substrate, incorporating membrane and bending capabilities, is here coupled with a three-dimensional array of nonlinear springs a-priori designed to be both elastically equivalent to the mechanical response of the bulky substrate and capable to somehow include the actual boundary conditions. In this way, under the hypothesis of perfect bond at the interface, the stretchable and flexible film kinematics depends on how the film middle surface elastically interacts with the support, whose behavior is to this end reduced to that of a three-dimensional network of nonlinear elastic springs derived by generalizing the Winkler-Pasternak foundation model through homogenization techniques [74–76].

In particular, the overall mechanical behavior of the substrate along the vertical (orthogonal to the film-substrate interfacial surface) and the horizontal (parallel to the interface) directions has been first obtained in closed-form in terms of out-of-plane and in-plane equivalent nonlinear stiffness properties, by implicitly taking into account the imposed constraints at the basis of the substrate. As mentioned above, this strategy allowed to avoid the extremely onerous computational costs required by other modeling approaches which, by coupling thick substrates to thin films, forced to solve a number of equations of the order of about 10^8, with additional time-consuming calculations needed to include nonlinearities. The generalized Winkler-Pasternak models were then specialized to bi-material strata, in the cases at hand the first being made of a polymeric (PDMS) layer and the other one of a stiffer (glass or Lithium Niobate, LN) substrate. Two different assumptions have been made to attribute proper stiffness values to the network springs families, by considering a transversal order of springs interlaced with vertically positioned ones obeying the Reuss-based (harmonic or sub-contrary mean) stiffness estimation representing the two materials met along the $z-$ direction. In what follows, the PDMS layer of thickness H_s is named *substrate* and denoted with the subscript s, while the subscript b (*basis*) refers to the stiffer bulky substrate materials, say glass or LN in our cases, whose thickness is $H_b = H - H_s$ (see Fig. 1(a)). Preliminary calculations lead to so find the stiffness constants as $K_s = E_s t L_0^{-1}$ and $K_b = E_b t L_0^{-1}$, E_s and E_b being the Young's moduli of the two strata and t the in plane depth of the system. Furthermore, by assuming perfect bound at $z = H$ and piecewise linear functions to describe the spring network lateral expansion, an energy-based procedure allowed to determine the overall transverse stiffness as (see Fig. 5(b))

$$\overline{K}_{\text{transv}} = \frac{H_s t}{12} \frac{E_s(4H\ E_b - 4\ H_s E_b + 3H_s E_s)}{L_0(H\ E_b + H_s(E_b - E_s))} \quad (4)$$

Coherently with several works [55,56,57,72], the nonlinear contribution of the polymeric PDMS layer was modeled by starting from a generalized neo-Hookean hyperelastic law, with the strain energy

function (SEF) written as $\Psi_{\text{NH}} = \frac{\mu_s}{2}(I_1 - 3) + \frac{\mu_s}{2\beta}(J^{-2\beta} - 1)$, with β

$= \frac{\nu_s}{1 - 2\nu_s}, \mu_s = \frac{E_s}{2(1 + \nu_s)}, I_1$ and J being respectively the first invariant of the right Cauchy-Green tensor and the Jacobian of the deformation gradient [77]. By following this way, for the generic $j-$th spring of the three-dimensional network one finally obtains the explicit expression of the nonlinear stiffness along the direction normal to the film-support interface as follows:

$$K_{norm} = K_{norm}^L$$
$$\times \frac{u_z\left(3L_j^2 + 3L_j u_z + u_z^2\right)}{3(L_j + u_z)^2}, \quad K_{norm}^L = 1/\left(\frac{(H_s L)}{E_s}\frac{1}{t} + \frac{(H - H_s)L}{E_b}\frac{1}{t}\right) \quad (5)$$

u_z being the displacement along the $z-$direction and L_j the equivalent spring length. The so defined neoHookean behavior is shown in Fig. 5(c), by considering material incompressibility and a spring length of about 4.8 μm representing the PDMS mean thickness.

At the end, a parametrical description of possible bas-reliefs has been considered to take into account the peculiar geometry of film-PDMS interface when the polymeric stratum is deposited on a non-flat solid substrate.

2.4. Finite element simulations

Numerical simulations have been conducted with the aid of the commercial FEM-based code ANSYS® [78], by first performing static analyses and including large deformations, homogenized hyperelastic behavior of the substrate and nonlinear post-buckling of the Aluminum film. To model the actual cases and to interpret the related experimental results, three types of geometries have been in particular considered: a *simple planar* surface and both so-called *micro-donut* and *micro-lens* shaped surfaces.

To model the surface imperfections and slight film thickness variability resulting from the technology used for deposition of thin aluminum layers on PDMS substrates [79], an automatic procedure was ad-hoc employed for randomly changing the thickness of each FE shell element, with thickness variation Δt_i ranging within the interval $(-\overline{t} \times 0.1, \overline{t} \times 0.1)$, $\overline{t}$ being the mean reference (nominal) thickness. The randomly generated film imperfections have been used to trigger instability phenomena prodromal to film wrinkling in the non-linear post-buckling simulation [80], by preliminarily checking the independence of eigenvalues and eigenvectors with respect to the random thickness variation assigned, to so avoid imperfection-guided deformation patterns [65] and prevent qualitatively false results. In particular, for obtaining faithful results, robustness of the modeling strategy and computational cost effectiveness of the numerical FE analyses, the minimum mesh size was roughly estimated through the value of critical wavelength expected from Eq. (2), by then considering at least four elements along each sinusoidal wave. In the case of 3D shaped substrata (lens and donuts), the rule-of-thumb above mentioned appeared to be not sufficiently accurate for predicting the proper number and size of finite elements and therefore preliminary numerical eigenvalue analyses were considered to evaluate the final model discretization.

Symmetry was exploited to further reduce computational costs when not interfering with non-symmetrical wrinkling patterns. As suggested by Cai et al. [65], a thermal load dropt ΔT_{NL} capable to put under compression the structure was then applied and the related thermal load amplification factor was evaluated through a preliminary eigenvalue buckling analysis. Finally, by essentially following the way suggested in [63] to avoid convergence problems, artificial damping forces were added to the equilibrium equations for stabilizing the wrinkling process.

In Fig. 6 the details of the geometries and the FE mesh parameterized are shown. In Fig. 6(a) 1D (spring) and 2D (shell with membrane and
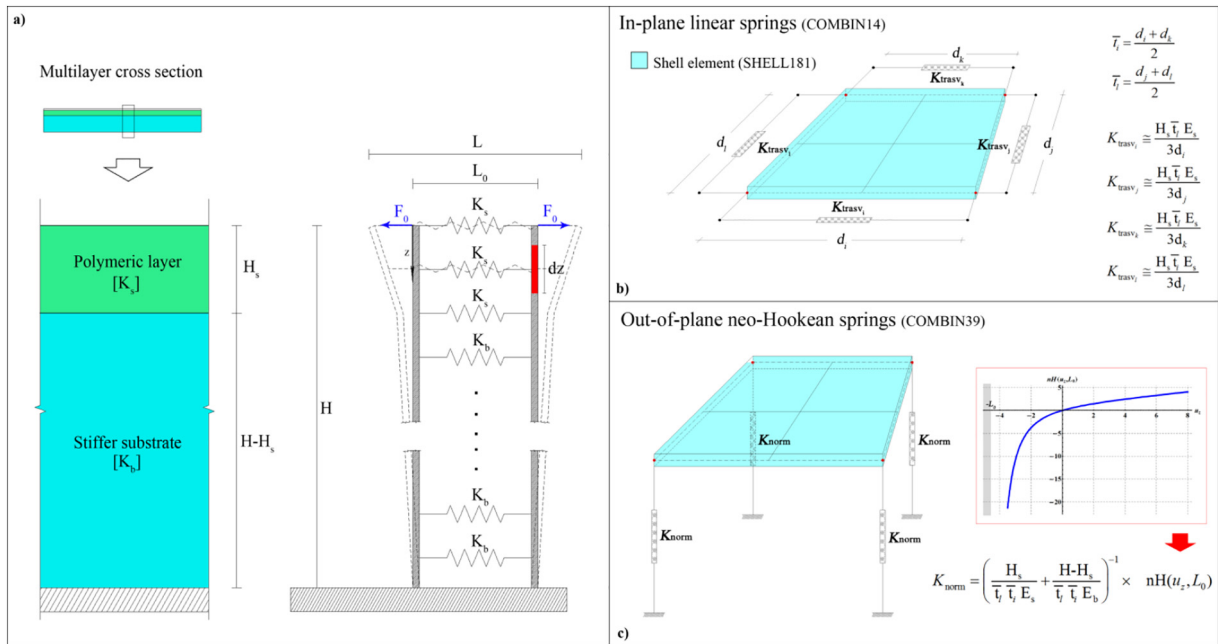
Fig. 5. Sketch of the hybrid analytical-numerical (FE) modeling approach: a) lateral view of the multilayer substrate (polymer and stiffer strata) with the at the basis constraint (left) and equivalent discrete system of in-parallel transversal springs incorporating strata stiffness and deformation modes compatible with the boundary conditions (right); generic Finite Element shell element (thin film) with in-plane (b) and out-of-plane (c) nonlinear springs accounting for the interaction of the thin film with the soft polymeric substrate.

bending features) finite elements and mesh adopted to replicate the 3D problem are described, while in Fig. 6(b) a zoom of the springs distribution to model film-substrate interfacial behavior is reported.

The zooming in Fig. 6(c, d) highlights the thickness imperfections obtained by lunching the already mentioned random procedure used for the previous analyses. As above, symmetrical boundary conditions were hence applied at the edges of the model, with the drop temperature ΔT_{NL} introduced to generate the in-plane compressive state condition, adopting an eigenvalue buckling analysis to estimate critical stress values. The geometry of the donuts and micro-bumps was virtually reconstructed in the simulation by cutting a sphere of radius R_{in} (see Fig. 6(e, f)), in this way preventing any discontinuity along the surface of revolution that could give rise incorrect strain localization and wrinkling onset.

3. Results and discussion

To analyze wrinkling occurring in thin aluminum films adhered on a thick compliant substrate induced by heating/cooling phenomena due to the film deposition process, nonlinear (post-buckling) numerical Finite Element-based (FEM) analyses were conducted in a 2D-3D hybrid way, that is by uploading the results obtained through the homogenization of the substrate elastic response derived by modeling it as a bed made of a three-dimensional network of nonlinear springs in the FE model of the thin film-substrate system.

The post-buckling behavior of a flat model was studied as first, to appreciate the capability of the proposed procedure to capture both the wrinkling onset and the deformation evolution. As previously said, a perfectly flat thin film model bonded on a 3D generalized Winkler-Pasternak nonlinearly elastic bed was thus considered, randomly generating a distribution of film thickness imperfections with amplitude Δt_i - initially set equal to 1 μm - to incorporate the actual inhomogeneous variation of the film thickness due to the deposition process that in turn will activate the post-buckling phenomenon. The results in terms of vertical displacements U_z are shown in Fig. 7, where it is also possible to follow how the instability-driven deformation profiles grow and organize as the overall compressive load increases in the film. Although the response has been verified to result as essentially

indifferent to the family of randomly generated film thickness imperfections in qualitative and quantitative terms, the results nevertheless suggested that the imperfection overall plays a crucial role in breaking the symmetry and triggering the out-of-plane bending deformation, also ensuring to not overestimating the actual critical compressive load at the onset of instability. The employment of both kinematical (large deformations) and constitutive (hyperelastic) nonlinearities into the simulation lead to reach the final equilibrium condition after 46 sub-steps, corresponding to about only few seconds of process by using a standard dual-core processor and a commercial PC machine. Around the *8-th* sub-step, the stress state in the film equates the compressive critical one and at early stage disordered and uniformly distributed wrinkle nuclei appeared as jeopardized blisters. As the load progressively increased, the isolated deformation bubbles ceased to be segregated, their boundaries growing and the minimum elastic energy driving close bent regions to intersect (see circled in red zones in the insets of Fig. 7), finally forming ordered albeit not symmetrical wrinkle patterns with clearly recognizable families of almost parallel wrinkles aligned in four main different directions. At the end, these patterns stabilize their drawing in a labyrinth-like shape, as well as the related average wavelength sizes, wrinkles slightly increasing in amplitude with different inward and outward displacement magnitudes, as somehow expected as a consequence of the hyperelasticity of the substrate (see Fig. 7, sub-step#46).The whole wrinkles formation process, i.e. 46 steps, is reported in Movie 1.

Our pattern morphological evolution can be compared with some literature results, obtained with other computational strategies, for instance by Huang et al. [62], in which, under biaxial compression, the film preferred a checkerboard wrinkling pattern at lower over-strain. Importantly, Fig. 7 shows that, by comparing theoretical outcomes with experimental findings, an essential agreement can be traced both in terms of wrinkle distributions (whose pathways are highlighted in dotted black and yellow lines for the numerical and experimental situations, respectively) and wavelengths, as explicitly indicated in the Fig. 7.

By following the analogous line of reasoning adopted for analyzing wrinkling in flat thin films, the nonlinear response of the *micro-donut* shaped model was then investigated (see Fig. 8). For this case, a thinner
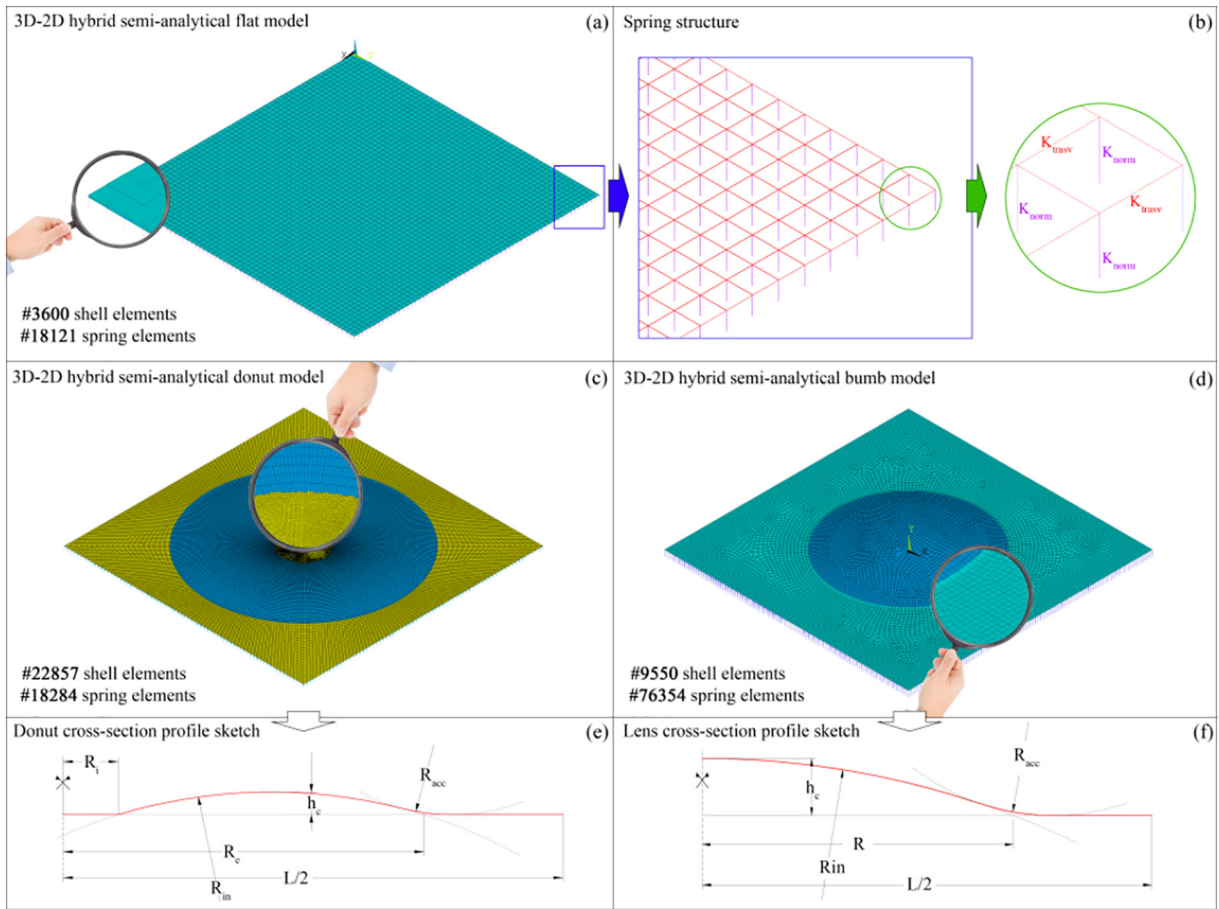
Fig. 6. Details of the geometries and the FE mesh parameterized: a) 1D (spring) and 2D (shell with membrane and bending features) finite elements and mesh adopted to replicate the 3D problem; b) distribution of the springs to model film-substrate interfacial behavior; "donut" (c) and "bump" (d) FE model and related geometrical parameterizations (e, f).
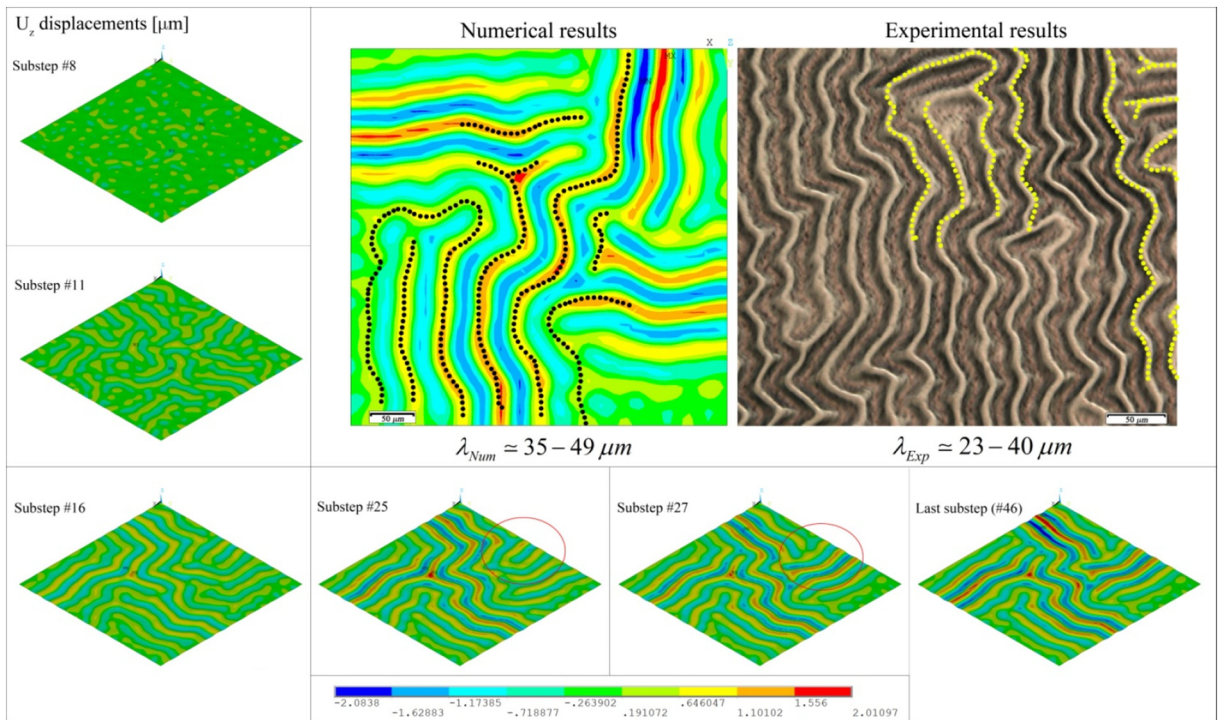

Fig. 7. Synoptic table of the hybrid modeling results for films on flat (glass) substrates: numerical (in silico FE simulations) vs experiments (top-right), where coherent wrinkling wavelengths and orographic profiles can be appreciated; sequence of the analysis sub-steps in terms of out-of-plane displacements, with random nucleation and progressive ordering of final wrinkles patterns (left and bottom sides).The entire process is shown in Movie 1.

film was considered with a thickness around 0.2 μm, preserving the regularity of the element shapes by using a finer element size to mesh the micro-donut surface. As highlighted by the zooming in the Fig. 8, the film thickness imperfections were again considered by randomly modulating a slightly oscillating value to take into account the real spatial film thickness variation intrinsically induced by the deposition process. Suitable symmetrical boundary conditions, compatible with both constraints and periodicity of the micro-donut shaped regions, were applied at the edges of the selected square unit and a temperature drop ΔT_{NL} was applied to the model for ingenerating in-plane compressive stress state conditions. The post-buckling response is shown in Fig. 8, where wrinkled micro-patterns formed during progressively increasing compressive loads can be appreciated. In this simulation the stable equilibrium condition was reached after 37 sub-steps: in particular, as highlighted by the sequence of images at different intermediate sub-steps (equivalent to time steps), the wrinkles start separately and almost consecutively to then move radially from the central zone and the outmost annulus of the donut (see sub-step #13 in Fig. 8). By obeying the minimum energy principle, these patterns gradually and simultaneously grow to invade the intermediate regions, successively connecting together starting from sub-step #20. The simulation highlighted a hierarchical generation of wrinkles - probably influenced by the curvature of the surface [82] - with unstable phenomena and ripples (see the zone circled by the red lines in Fig. 8) that at the end progressively stabilize by drawing the patterns shown in the figure. The complete sequence is shown in Movie 2.

As in the previously case, the numerical results were compared with the experimental ones, registering agreement both in terms of wavelengths and wrinkling shapes, as highlighted by means of the yellow and red dotted lines in Fig. 8. It is worth to notice that, as seen in the zoom in Fig. 8, the wave patterns run along several directions: from the center to the donut outer radius, the waves mainly run radially, whereas hoop-directed waves form along the internal and the external donut circumferences, smaller radial patterns starting and smoothly

vanishing from the external donut fence by approaching larger areas with no wrinkles.

To verify that the imposed symmetrical boundary conditions applied to this numerical model and the choice of the periodic unit did not affect the results in terms of wrinkling shapes and characteristic wavelengths, a further FE model was developed by selecting a different modulus of the donut-shaped periodic structure, then applying to it symmetrical boundary conditions at the edges, as well as the same loads of the complementary case already studied. The results are shown in Fig. 9. Therein, it is possible to observe that, in both the modeling cases of Figs. 8 and 9, the wrinkling patterns are found to be essentially the same and the outcomes well replicate the actual experimental deformation profiles, as highlighted in the second case through the yellow and the blue dashed lines.

Finally, a nonlinear post-buckling analysis was performed for the *micro-lens* model in which the geometrical setting, shown in Fig. 10, was developed according to the experimental measures. On the basis of the geometry of the surfaces, to avoid significant errors in predicting wrinkling formation, particular attention was devoted in this case for determining the maximum element size in according to the expected wavelength value, here a priori evaluated by means of the rough analytical equation available in the literature, by considering an aluminum thin film with a thickness of about 0.2 μm deposited on a PDMS substrate.

Under the drop temperature considered, the equilibrium condition was reached after 65 sub-steps (see Movie 3). The results showed two main families of waves: one made of a radial pattern starting from the outer side of the lens and another characterized by somehow concentric waves invading the central region of the lens, with decreasing amplitude from the outer to the inner part of the lens, but essentially preserving the same constant wavelength. The time-histories of these patterns can be appreciated by following the sequence of images reported in Fig. 10. Therein, a first instability phenomenon starts on the circular edge of the lens (see substep #4), then new wave patterns extend
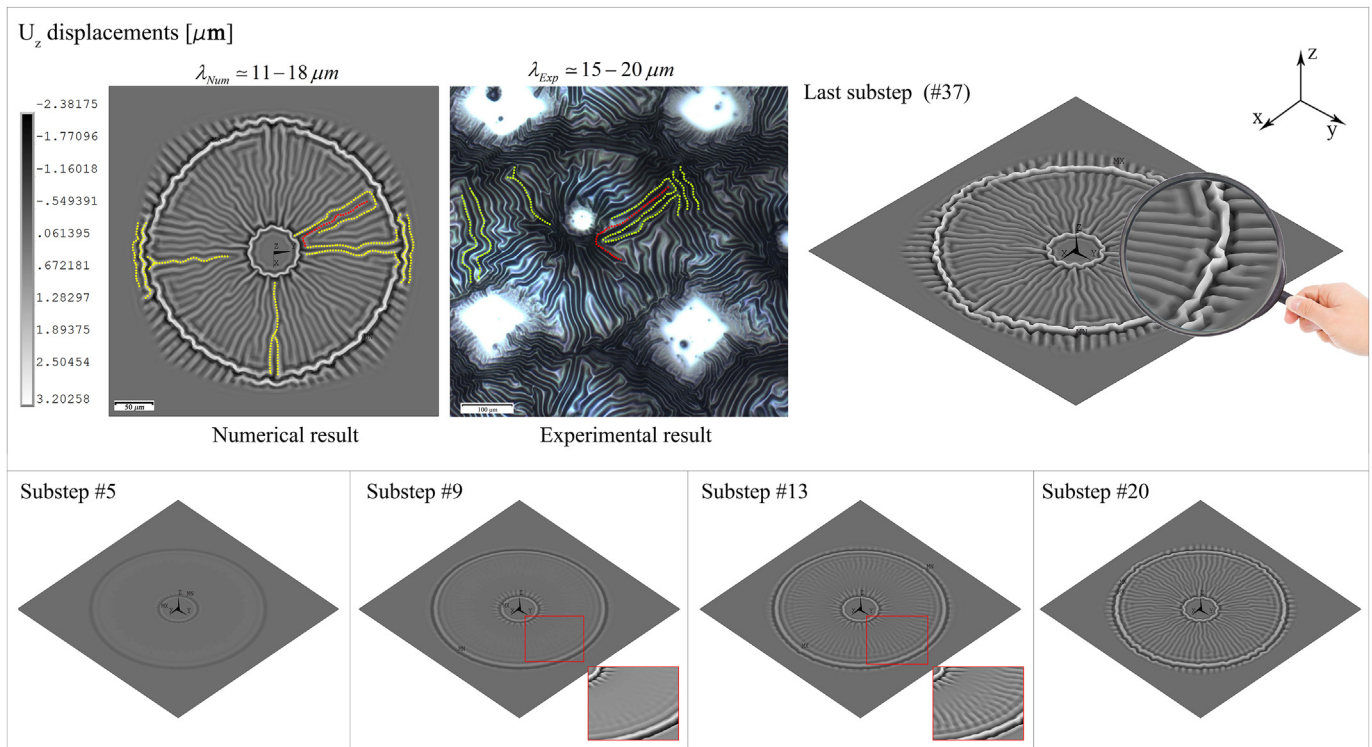

Fig. 8. Synoptic table of the hybrid modeling results for films on PPLN/elastomer donut-shaped substrates: numerical (in silico FE simulations) vs experiments (top-left), with a particular of the wrinkled structure (top-right), in which coherent wrinkling wavelengths and details of orographic patterns can be visualized; sequence of the analysis substeps in terms of out-of-plane displacements (from Movie 2), with localized wrinkles onset and evolution towards the final topologies (bottom).

radially (see substep #8 to #15), successively doubling/splitting when their length increases (see Fig. 10, sub-steps from #25 to #55) [81–82]. Additional remarks can be made by observing how the hoop waves, during the progressive compressive load increase, tend to separate, this being probably at the basis of the wave fragmentation inside the lens resulting from the experimental evidences. By comparing the theoretical outcomes with the experimental ones, a substantial agreement can be still established between them in terms of wrinkling patterns and quantitatively, by measuring the corresponding wavelengths. Apart from the formation and the evolution of the wrinkles, it is worth to highlight that the numerical modeling well captures a crucial feature of the actual system response, that is the polygonal shape that tends to assume the wrinkles drawing around the lens border, a fact that supports the effectiveness of the proposed strategy in catching actual behaviors that the symmetry of the problem otherwise would obscure and the sole eigenvalue analyses could not recognize.

4. Conclusions

In this work we have shown metal wrinkling formation on PDMS flat as well as complex structures built up on PPLN substrates. These patterns and their evolution in time seem to be well predicted by the proposed hybrid analytical-numerical approach. The results reported here demonstrate that onset of instability, wrinkling formation and evolution in thin metal films on flat surfaces, as well as in presence of surfaces with periodic three-dimensional profiles, can be all predicted with sufficiently good accuracy and relatively modest computational costs by introducing a hybrid strategy in which the film-substrate interaction is obtained by uploading in a Finite Element model an ad hoc conceived three-dimensional network of nonlinear springs of which the analytical response is derived by means of a homogenization procedure incorporating the boundary conditions. The theoretically obtained outcomes from numerical simulations for three different and relevant cases of interest, compared with the corresponding experimental results, have shown the actual capability of the procedure to catch both qualitative and quantitative features of the response of the systems. Noteworthy, the intermediate stages of the progressive evolution of complex wrinkling patterns were also achieved, these phenomena generally remaining unpredictable by the sole weapons of the classical eigenvalues analysis. We believe that the proposed strategy might be helpfully utilized for predicting hierarchical organizations of wrinkle drawings, analyzing post-buckling phenomena in thin films governed
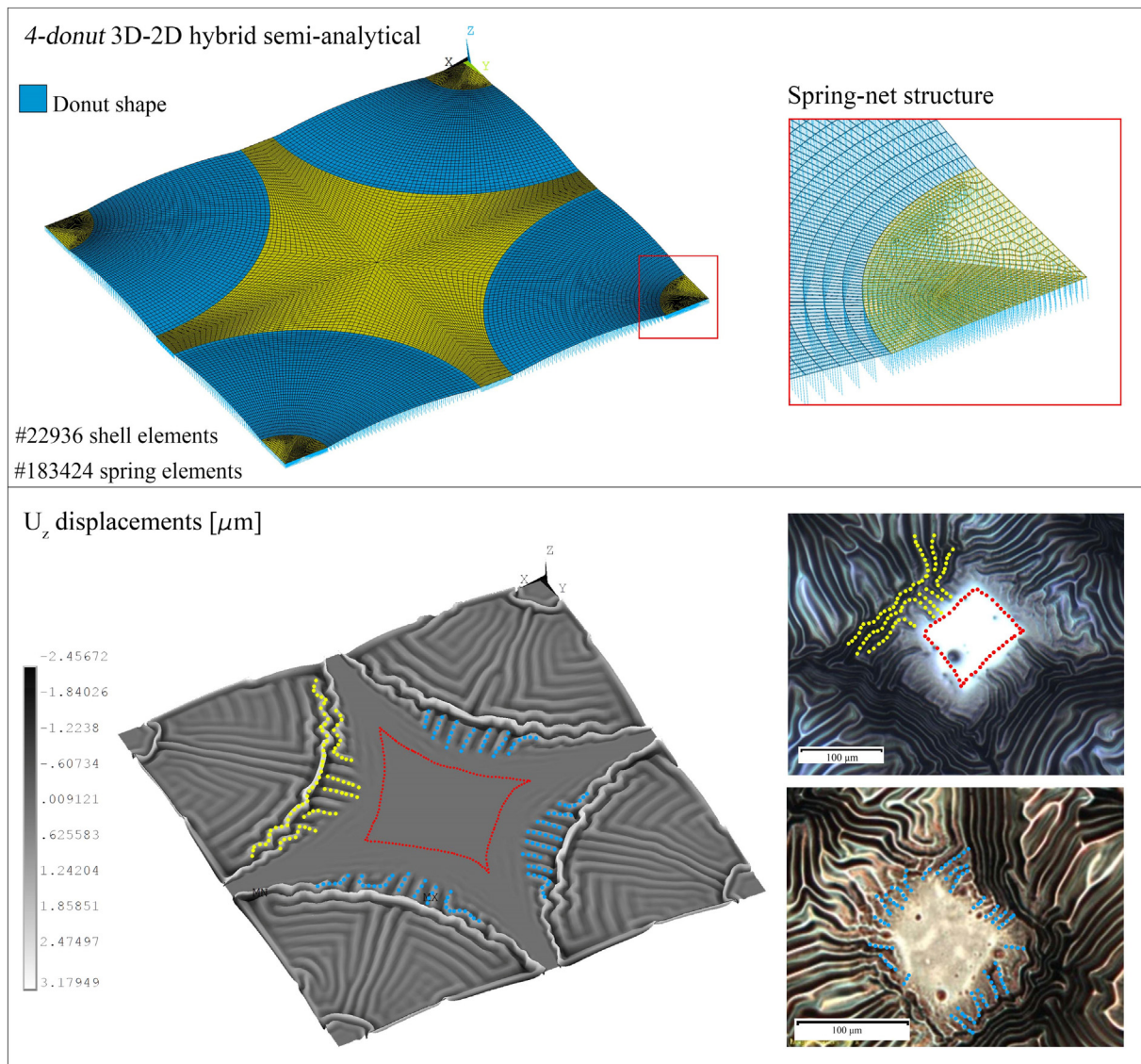

Fig. 9. Results from hybrid modeling of films on donut-shaped substrates by considering a different unit of the same structure as in Fig. 6: the results in terms of pattern formation and evolution essentially replicate those already illustrated in Fig. 6, highlighting the effectiveness and the robustness of the proposed strategy which does not depend on the "window" selected to analyze the problem for periodically arranged structures.
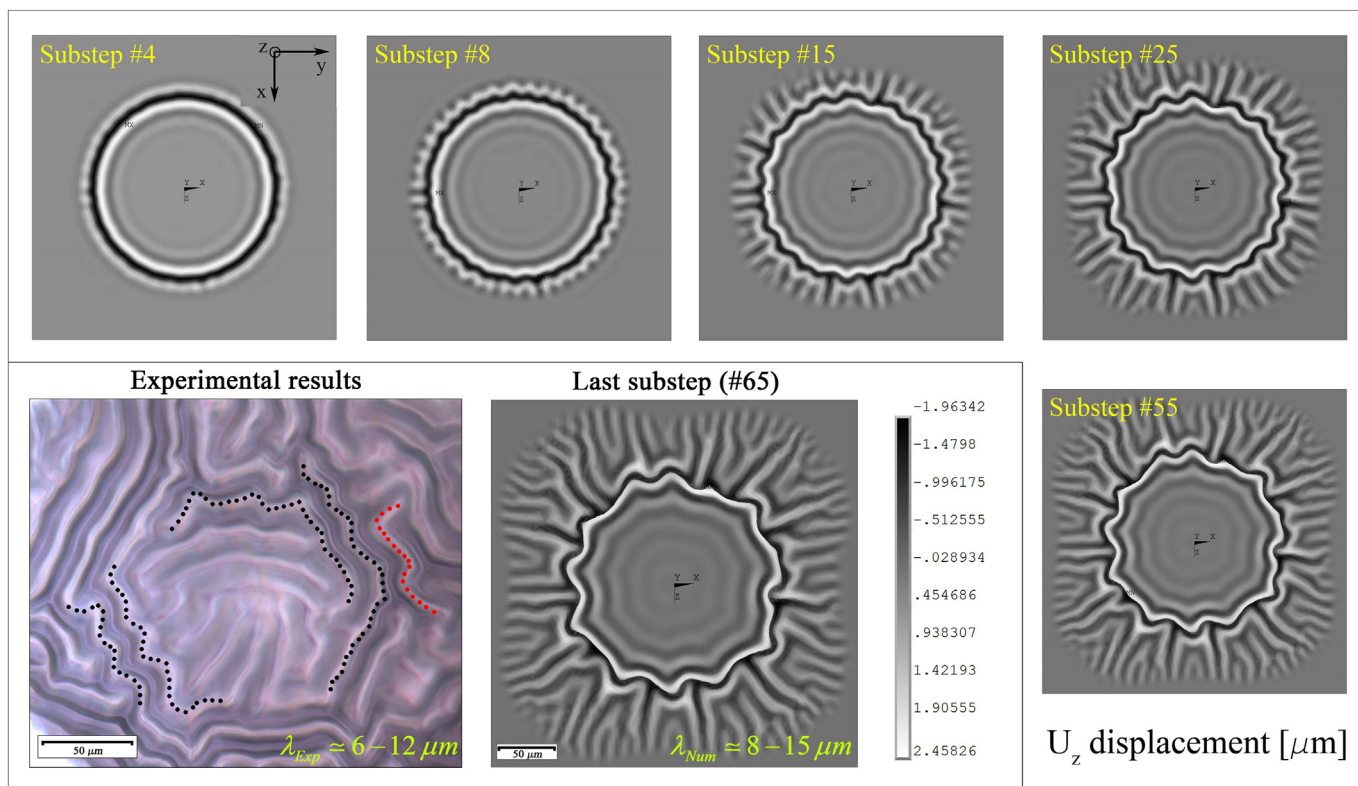
Fig. 10. Synoptic table of the hybrid modeling results for films on bump-shaped substrates: experiments (bottom-left) vs FE simulations (bottom-right), with the sequence of the analysis substeps showing of out-of-plane displacements, from the formation to final orography (top and right), reported in Movies 3.

by multi-physics events and envisaging optimization protocols to design special wrinkling-folding structures at different scale levels, by so paving the way for valid alternatives to 3D printing and other related emerging procedures to construct micro- or nano-curved surfaces for several engineering applications.

Supplementary data to this article can be found online at https://doi.org/10.1016/j.matdes.2019.108314.

Author contributions

The manuscript was written through contributions of all authors. All authors have given approval to the final version of the manuscript.

CRediT authorship contribution statement

A. Cutolo: Software, Formal analysis. **V. Pagliarulo:** Investigation, Methodology, Data curation. **F. Merola:** Investigation, Methodology, Data curation. **S. Coppola:** Validation. **P. Ferraro:** Supervision, Conceptualization, Writing - review & editing. **M. Fraldi:** Conceptualization, Writing - review & editing.

Declaration of competing interest

The authors declare that they have no known competing financial interests or personal relationships that could have appeared to influence the work reported in this paper.

References

[1] Y. Sun, W.M. Choi, H. Jiang, Y.Y. Huang, J.A. Rogers, Controlled buckling of semiconductor nanoribbons for stretchable electronics, Nat. Nanotechnol. (2006) https://doi.org/10.1038/nnano.2006.131.

[2] S. Baek, H. Jang, S.Y. Kim, H. Jeong, S. Han, Y. Jang, D.H. Kim, H.S. Lee, Flexible Piezocapacitive Sensors Based on Wrinkled Microstructures: Toward Low-cost Fabrication of Pressure Sensors Over Large Areas, 2017 https://doi.org/10.1039/C7RA06997A.

[3] Y. Li, Reversible wrinkles of monolayer graphene on a polymer substrate: toward stretchable and flexible electronics, Soft Matter (2016) https://doi.org/10.1039/C6SM00108D.

[4] N.R. Visaveliya, C.W. Leishman, K. Ng, N. Yehya, N. Tobar, D.M. Eisele, J.M. Köhler, Adv. Mater. Interfaces (2017) https://doi.org/10.1002/admi.201700929.

[5] Y. Tokudome, H. Kuniwaki, K. Suzuki, D. Carboni, G. Poologasundarampillai, M. Takahashi, Thermoresponsive wrinkles on hydrogels for soft actuators, Adv. Mater. Interfaces (2016) https://doi.org/10.1002/admi.201500802.

[6] H.W. Hu, G. Haider, Y.M. Liao, P.K. Roy, R. Ravindranath, H.T. Chang, C.H. Lu, C.Y. Tseng, T.Y. Lin, W.H. Shih, Y.F. Chen, Wrinkled 2D materials: a versatile platform for low-threshold stretchable random lasers, Adv. Mater. (2017) https://doi.org/10.1002/adma.201703549.

[7] X. Cheng, B. Meng, X. Chen, M. Han, H. Chen, Z. Su, M. Shi, H. Zhang, Single-step fluorocarbon plasma treatment-induced wrinkle structure for high-performance triboelectric nanogenerator, Small (2016) https://doi.org/10.1002/smll.201502720.

[8] S.Y. Ryu, J.H. Seo, H. Hafeez, M. Song, J.Y. Shin, D.H. Kim, Y.C. Jung, C.S. Kim, Effects of the wrinkle structure and flat structure formed during static low-temperature annealing of ZnO on the performance of inverted polymer solar cells, J. Phys. Chem. C (2017) https://doi.org/10.1021/acs.jpcc.7b02149.

[9] E. Plancher, L. Héraud, P. Lhuissier, R. Dendievel, D. Fabrègue, J.J. Blandin, G. Martin, Towards behavior by design: a case study on corrugated architectures, Mater. Des. 166 (2019) https://doi.org/10.1016/j.matdes.2019.107604.

[10] J.B. Kim, P. Kim, N.C. Pégard, S.J. Oh, C.R. Kagan, J.W. Fleischer, H.A. Stone, Y.L. Loo, Wrinkles and deep folds as photonic structures in photovoltaics, Nat. Photonics (2012) https://doi.org/10.1038/nphoton.2012.70.

[11] J. Lin, J. Zhong, S. Zhong, H. Li, H. Zhang, W. Chen, Modulating electronic transport properties of MoS$_2$ field effect transistor by surface overlayers, Appl. Phys. Lett. (2013) https://doi.org/10.1063/1.4818463.

[12] W.H. Koo, S.M. Jeong, F. Araoka, K. Ishikawa, S. Nishimura, T. Toyooka, H. Takezoe, Light extraction from organic light-emitting diodes enhanced by spontaneously formed buckles, Nat. Photonics (2010) https://doi.org/10.1038/nphoton.2010.7.

[13] J.Y. Chung, A.J. Nolte, C.M. Stafford, Surface wrinkling: a versatile platform for measuring thin-film properties, Adv. Mater. (2011) https://doi.org/10.1002/adma.201001759.

[14] D.H. Kim, J.H. Ahn, W.M. Choi, H.S. Kim, T.H. Kim, J. Song, Y.Y. Huang, Z. Liu, C. Lu, J.A. Rogers, Stretchable and foldable silicon integrated circuits, Science 320 (5875) (2008) 507–511, https://doi.org/10.1126/science.1154367. http://science.sciencemag.org/content/320/5875/507.

[15] P.J. Yoo, H.H. Lee, Morphological diagram for metal/polymer bilayer wrinkling: influence of thermomechanical properties of polymer layer, Macromolecules (2005) https://doi.org/10.1021/ma048452.

[16] S. Schauer, M. Worgull, H. Hölscher, Bio-inspired hierarchical micro- and nano-wrinkles obtained via mechanically directed self-assembly on shape-memory polymers, Soft Matter (2017) https://doi.org/10.1039/C7SM00154A.

[17] H. Godaba, Z.Q. Zhang, U. Gupta, C. Chiang Foo, J. Zhu, Dynamic pattern of wrinkles in a dielectric elastomer, Soft Matter (2017) https://doi.org/10.1039/C7SM00198C.

[18] W.T.S. Huck, N. Bowden, P. Onck, T. Pardoen, J.W. Hutchinson, G.M. Whitesides, Ordering of spontaneously formed buckles on planar surfaces, Langmuir (2000) https://doi.org/10.1021/la991302l.

[19] T. Ma, H. Liang, G. Chen, B. Poon, H. Jiang, H. Yu, Micro-strain sensing using wrinkled stiff thin films on soft substrates as tunable optical grating, Opt. Express (2013) https://doi.org/10.1364/OE.21.011994.

[20] M. Nania, F. Foglia, O.K. Matar, J.T. Cabral, Sub-100 nm wrinkling of polydimethylsiloxane by double frontal oxidation, Nanoscale (2017) https://doi.org/10.1039/C6NR08255F.

[21] N. Bowden, S. Brittain, A.G. Evans, J.W. Hutchinson, G.M. Whitesides, Spontaneous formation of ordered structures in thin films of metals supported on an elastomeric polymer, Nature (1998) https://doi.org/10.1038/30193.

[22] W.Y. Zhang, J.P. Labukas, S. Tatic-Lucic, L. Larson, T. Bannuru, R.P. Vinci, G.S. Ferguson, Novel room-temperature first-level packaging process for microscale devices, Sensors Actuators A Phys. (2005) https://doi.org/10.1016/j.sna.2005.03.008.

[23] Y. Yan, X. Ha, W. Din, S. Jian, Y. Ca, C. Lu, Controlled free edge effects in surface wrinkling via combination of external straining and selective O₂ plasma exposure, Langmuir (2013) https://doi.org/10.1021/la4010517.

[24] J. Yin, J.L. Yagüe, D. Eggenspieler, K.K. Gleason, M.C. Boyce, Deterministic order in surface micro-topologies through sequential wrinkling, Adv. Mater. (2012) https://doi.org/10.1002/adma.201201937.

[25] F. Brau, P. Damman, H. Diamant, T.A. Witten, Wrinkle to fold transition: influence of the substrate response, Soft Matter (2013) https://doi.org/10.1039/C3SM50655J.

[26] E.S. Sung, H.C. Gwan, Y. Gi-Ra, J.Y. Pil, Competitive concurrence of surface wrinkling and dewetting of liquid crystalline polymer films on non-wettable substrates, Soft Matter (2017) https://doi.org/10.1039/C7SM01668A.

[27] C. Androulidakis, E.N. Koukaras, M.P. Carbone, M. Hadjinicolaou, C. Galiotis, Wrinkling formation in simply-supported graphenes under tension and compression loadings, Nanoscale (2017) https://doi.org/10.1039/C7NR06463B.

[28] W.K. Lee, J. Kang, K.S. Chen, C.J. Engel, W.B. Jung, D. Rhee, T.W. Odom, Multiscale, hierarchical patterning of graphene by conformal wrinkling, Nano Lett. (2016) https://doi.org/10.1021/acs.nanolett.6b03415.

[29] S. Coppola, G. Nasti, V. Vespini, L. Mecozzi, R. Castaldo, G. Gentile, M. Ventre, P.A. Netti, P. Ferraro, Quick liquid packaging: encasing water silhouettes by three-dimensional polymer membranes, Sci. Adv. (2019) https://doi.org/10.1126/sciadv.aat5189.

[30] W.B. Jung, K.M. Cho, W.K. Lee, T.W. Odom, H.T. Jung, Universal method for creating hierarchical wrinkles on thin-film surfaces, ACS Appl. Mater. Interfaces (2017) https://doi.org/10.1021/acsami.7b14011.

[31] H.C. Jeong, H.G. Park, Y.H. Jung, J.H. Lee, B.Y. Oh, D.S. Seo, Tailoring the orientation and periodicity of wrinkles using ion-beam bombardment, Langmuir (2016) https://doi.org/10.1021/acs.langmuir.6b01473.

[32] D. Wang, N. Cheewaruangroj, Y. Li, G. McHale, Y. Jiang, D. Wood, J.S. Biggins, B.B. Xu, Spatially configuring wrinkle pattern and multiscale surface evolution with structural confinement, Adv. Funct. Mater. (2018) https://doi.org/10.1002/adfm.201704228.

[33] A. Das, A. Banerji, R. Mukherjee, Programming feature size in the thermal wrinkling of metal polymer bilayer by modulating substrate viscoelasticity, ACS Appl. Mater. Interfaces (2017) https://doi.org/10.1021/acsami.7b08333.

[34] A. Nogales, A. Del Campo, T.A. Ezquerra, J. Rodriguez-Hernández, Wrinkling and folding on patched elastic surfaces: modulation of the chemistry and pattern size of microwrinkled surfaces, ACS Appl. Mater. Interfaces (2017) https://doi.org/10.1021/acsami.7b03161.

[35] W.K. Lee, C.J. Engel, M.D. Huntington, J. Hu, T.W. Odom, Controlled three-dimensional hierarchical structuring by memory-based, sequential wrinkling, Nano Lett. (2015) https://doi.org/10.1021/acs.nanolett.5b02394.

[36] S. Zeng, R. Li, S.G. Freire, V.M. Garbellotto, E.Y. Huang, A.T. Smith, C. Hu, W.R.T. Tait, Z. Bian, G. Zheng, D. Zhang, L. Sun, Moisture-responsive wrinkling surfaces with tunable dynamics, Adv. Mater. (2017) https://doi.org/10.1002/adma.201700828.

[37] S. Hiltl, A. Böker, Wetting phenomena on (gradient) wrinkle substrates, Langmuir (2016) https://doi.org/10.1021/acs.langmuir.6b02364.

[38] C. Zong, Y. Zhao, H. Ji, X. Han, J. Xie, J. Wang, Y. Cao, S. Jiang, C. Lu, Tuning and erasing surface wrinkles by reversible visible-light-induced photoisomerization, Angew. Chem. (2016) https://doi.org/10.1002/ange.201510796.

[39] F. Xu, M. Potier-Ferry, Quantitative predictions of diverse wrinkling patterns in film/substrate systems, Sci. Rep. (2017) https://doi.org/10.1038/s41598-017-18267-0.

[40] A.V. Thomas, B.C. Andow, S. Suresh, O. Eksik, J. Yin, A.H. Dyson, N. Koratkar, Controlled crumpling of graphene oxide films for tunable optical transmittance, Adv. Mater. (2015) https://doi.org/10.1002/adma.201405821.

[41] F. Merola, M. Paturzo, S. Coppola, V. Vespini, P. Ferraro, Self-patterning of a polydimethylsiloxane microlens array on functionalized substrates and characterization by digital holography, J. Micromech. Microeng. (2009) https://doi.org/10.1088/0960-1317/19/12/125006.

[42] S. Coppola, V. Vespini, F. Olivieri, G. Nasti, M. Todino, B. Mandracchia, V. Pagliarulo, P. Ferraro, Direct self-assembling and patterning of semiconductor quantum dots on transferable elastomer layer, Appl. Surf. Sci. (2017) https://doi.org/10.1016/j.apsusc.2016.12.071.

[43] O. Gennari, R. Rega, M. Mugnano, E. Oleandro, L. Mecozzi, V. Pagliarulo, E. Mazzon, A. Bramanti, A. Vettoliere, C. Granata, P. Ferraro, S. Grilli, A skin-over-liquid platform with compliant microbumps actuated by pyro-EHD pressure, NPG Asia Materials (2019) https://doi.org/10.1038/s41427-018-0100-z.

[44] A. Marino, G. Ciofani, C. Filippeschi, M. Pellegrino, M. Pellegrini, P. Orsini, M. Pasqualetti, V. Mattoli, B. Mazzolai, Two-photon polymerization of sub-micrometric patterned surfaces: investigation of cell-substrate interactions and improved differentiation of neuron-like cells, ACS Appl. Mater. Interfaces (2013) https://doi.org/10.1021/am403895k.

[45] S. Coppola, G. Nasti, B. Mandracchia, V. Vespini, S. Grilli, V. Pagliarulo, P. Pareo, M. Manca, L. Carbone, G. Gigli, P. Ferraro, Two fold self-assembling of nanocrystals into nanocomposite polymer, IEEE Journal of Selected Topics in Quantum Electronics (2016) https://doi.org/10.1109/JSTQE.2015.2449657.

[46] M. Paturzo, F. Merola, P. Ferraro, Multi-imaging capabilities of a 2D diffraction grating in combination with digital holography, Opt. Lett. (2010) https://doi.org/10.1364/OL.35.001010.

[47] V. Vespini, O. Gennari, S. Coppola, G. Nasti, L. Mecozzi, V. Pagliarulo, S. Grilli, P. Ferraro, Electrohydrodynamic assembly of multiscale PDMS microlens arrays, IEEE Journal of Selected Topics in Quantum Electronics (2014) https://doi.org/10.1109/JSTQE.2014.2367656.

[48] F. Merola, S. Grilli, S. Coppola, V. Vespini, S. De Nicola, P. Maddalena, C. Carfagna, P. Ferraro, Reversible fragmentation and self-assembling of nematic liquid crystal droplets on functionalized pyroelectric substrates, Adv. Funct. Mater. (2012) https://doi.org/10.1002/adfm.201200323.

[49] F. Merola, S. Coppola, V. Vespini, S. Grilli, P. Ferraro, Characterization of Bessel beams generated by polymeric microaxicons, Meas. Sci. Technol. (2012) https://doi.org/10.1088/0957-0233/23/6/065204.

[50] V. Pagliarulo, O. Gennari, R. Rega, L. Mecozzi, S. Grilli, P. Ferraro, Twice electric field poling for engineering multiperiodic Hex-PPLN microstructures, Opt. Lasers Eng. (2018) https://doi.org/10.1016/j.optlaseng.2017.08.015.

[51] D. van den Ende, J.D. Kamminga, A. Boersma, T. Andritsch, P.G. Steeneken, Voltage-controlled surface wrinkling of elastomeric coatings, Adv. Mater. (2013) https://doi.org/10.1002/adma.201300459.

[52] B. Sarkar, D.K. Satapathy, M. Jaiswal, Wrinkle and crack-dependent charge transport in a uniaxially strained conducting polymer film on a flexible substrate, Soft Matter (2017) https://doi.org/10.1039/C7SM00972K.

[53] B. Osmani, H. Deyhle, T. Töpper, T. Pfohl, B. Müller, Gold layers on elastomers near the critical stress regime, Advanced Materials Technologies (2017) https://doi.org/10.1002/admt.201700105.

[54] Al-Rashed H., Lòpez J.F., Marthelot J., Reis P.M. "Buckling patterns in biaxially pre-stretched bilayer shells: wrinkles, creases, folds and fracture-like ridges", Soft Matter, doi:https://doi.org/10.1039/C7SM01828B.

[55] J.W. Hutchinson, The role of nonlinear substrate elasticity in the wrinkling of thin films, Philos. Trans. R. Soc. A Math. Phys. Eng. Sci. (2013) https://doi.org/10.1098/rsta.2012.0422.

[56] Y. Cao, J.W. Hutchinson, Wrinkling phenomena in Neo-Hookean film/substrate bilayers, J. Appl. Mech. (2012) https://doi.org/10.1115/1.4005960.

[57] J.W. Hutchinson, Mechanics of Thin Films and Multilayer, Technical University of Denmark, 1996 1996.

[58] S.P. Timoshenko, J.M. Gere, Theory of Elastic Stability, McGraw-Hill, New York, 1961.

[59] X. Chen, J.W. Hutchinson, Herringbone buckling patterns of compressed thin films on compliant substrates, J. Appl. Mech. (2004) https://doi.org/10.1115/1.1756141.

[60] J. Liu, K. Bertoldi, Bloch wave approach for the analysis of sequential bifurcations in bilayer structures, Proceedings of the Royal Society A: Mathematical, Physical and Engineering Sciences (2015) https://doi.org/10.1098/rspa.2015.0493.

[61] A. Auguste, L. Jin, Z. Suo, R.C. Hayward, The role of substrate pre-stretch in post-wrinkling bifurcations, Soft Matter (2014) https://doi.org/10.1039/C4SM01038H.

[62] X. Huang, B. Li, W. Hong, Y.P. Cao, X.Q. Feng, Effects of tension–compression asymmetry on the surface wrinkling of film–substrate systems, Journal of the Mechanics and Physics of Solids (2016) https://doi.org/10.1016/j.jmps.2016.04.014.

[63] J.Y. Sun, S. Xia, M.W. Moon, K.H. Oh, K.S. Kim, Folding wrinkles of a thin stiff layer on a soft substrate, Proceedings of the Royal Society A: Mathematical, Physical and Engineering Sciences (2011) https://doi.org/10.1098/rspa.2011.0567.

[64] J. Zang, X. Zhao, Y. Cao, J.W. Hutchinson, Localized ridge wrinkling of stiff films on compliant substrates, J.Mech Phys Solids 60 (2012) 1265.

[65] S. Cai, D. Breid, A.J. Crosby, Z. Suo, J.W. Hutchinson, Periodic patterns and energy states of buckled films on compliant substrates, Journal of the Mechanics and Physics of Solids (2011) https://doi.org/10.1016/j.jmps.2011.02.001.

[66] F. Xu, M. Potier-Ferry, S. Belouettar, Y. Cong, 3D finite element modeling for instabilities in thin films on soft substrates, Int. J. Solids Struct. (2014) https://doi.org/10.1016/j.ijsolstr.2014.06.023.

[67] F. Xu, T. Wang, C. Fu, Y. Cong, Y. Huo, M. Potier-Ferry, Post-buckling evolution of wavy patterns in trapezoidal film/substrate bilayers, International Journal of Non-Linear Mechanics (2017) https://doi.org/10.1038/nnano.2006.131.

[68] Y. Sun, W.M. Choi, H. Jiang, Y.Y. Huang, J.A. Rogers, Controlled buckling of semiconductor nanoribbons for stretchable electronics, Nat. Nanotechnol. (2006) https://doi.org/10.1038/nnano.2006.131.

[69] N. Bowden, S. Brittain, A.G. Evans, J.W. Hutchinson, G.M. Whitesides, Spontaneous formation of ordered structures in thin films of metals supported on an elastomeric polymer, Nature (1998) https://doi.org/10.1038/30193.

[70] H.W. Hu, G. Haider, Y.M. Liao, P.K. Roy, R. Ravindranath, H.T. Chang, C.H. Lu, C.Y. Tseng, T.Y. Lin, Wei-Heng, Y.F. Chen, Wrinkled 2D materials: a versatile platform for low-threshold stretchable random lasers, Adv. Mater. (2017) https://doi.org/10.1002/adma.201703549.

[71] P.J. Yoo, K.Y. Suh, S.Y. Park, H.H. Lee, Physical self-assembly of microstructures by anisotropic buckling, Adv. Mater. (2002) https://doi.org/10.1002/1521-4095(20021002)14:19<1383::AID-ADMA1383>3.0.CO;2-D.

[72] Z.C. Shao, Y. Zhao, W. Zhang, Y. Cao, X.Q. Feng, Curvature induced hierarchical wrinkling patterns in soft bilayers, Soft Matter (2016) https://doi.org/10.1039/C6SM01088A.

[73] X. Chen, J. Yin, Buckling patterns of thin films on curved compliant substrates with applications to morphogenesis and three-dimensional micro-fabrication, Soft Matter (2010) https://doi.org/10.1039/C0SM00401D.

[74] W.T. Huck, N. Bowden, P. Onck, T. Pardoen, J.W. Hutchinson, G.M. Whitesides, Ordering of spontaneously formed buckles on planar surfaces, Langmuir (2000) https://doi.org/10.1021/la991302l.

[75] Z. Huang, W. Hong, Z. Suo, Evolution of wrinkles in hard films on soft substrates, Phys. Rev. E (2004) https://doi.org/10.1103/PhysRevE.70.030601.

[76] B. Audoly, Localized buckling of a floating elastica, Phys. Rev. E (2011) https://doi.org/10.1103/PhysRevE.84.011605.

[77] G.A. Holzapfel, Nonlinear solid mechanics: a continuum approach for engineering science, Meccanica (2002) https://doi.org/10.1023/A:1020843529530.

[78] ANSYS, Inc, ANSYS Mechanical User's Guide, release 15.0 Edition.

[79] K. Bordo, H.G. Rubahn, Effect of deposition rate on structure and surface morphology of thin evaporated Al films on dielectrics and semiconductors, Mater. Sci. (2012) https://doi.org/10.5755/j01.ms.18.4.3088.

[80] Y. Zhao, Y. Cao, W. Hong, M.K. Wadee, X.Q. Feng, Towards a quantitative understanding of period-doubling wrinkling patterns occurring in film/substrate bilayer systems, Proceedings of the Royal Society A: Mathematical, Physical and Engineering Sciences (2015) https://doi.org/10.1098/rspa.2014.069.

[81] Vandeparre H, Gabriele S, Brau F, Gay C, Parker KK and Damman P. "Hierarchical wrinkling patterns", Soft Matter doi:https://doi.org/10.1039/C0SM00394H.

[82] Fraldi M, Cutolo A, Esposito L, Perrella G, Pastore Carbone MG, Sansone L, Scherillo G and Mensitieri G."Delamination onset and design criteria of multilayer flexible packaging under high pressure treatments", Innovative Food Sci. Emerg. Technol.. doi: https://doi.org/10.1016/j.ifset.2014.02.016.